Colloid Polym Sci (2008) 286:385–394
DOI 10.1007/s00396-007-1778-6

ORIGINAL CONTRIBUTION

Sedimentation and drying dissipative patterns of binary suspensions of colloidal silica spheres having different sizes

Tsuneo Okubo · Junichi Okamoto · Akira Tsuchida

Received: 10 August 2007 / Revised: 28 September 2007 / Accepted: 29 September 2007 / Published online: 8 November 2007

Abstract The sedimentation and drying dissipative structural patterns were formed during the course of drying binary mixtures among colloidal silica spheres of 183 nm, 305 nm, and 1.205 μm in diameter in aqueous suspension on a watch glass, a glass dish, and a cover glass, respectively. The broad ring-like sedimentation patterns were formed within several hours in suspension state for all the substrates used. Colorful macroscopic broad ring-like drying patterns were formed for the three substrates. In a watch glass, macroscopic drying patterns were composed of the outer and inner layers of small and large spheres, respectively. The two colored layers were ascribed to the Bragg diffractions of light by the dried colloidal crystals of the corresponding spheres. The width ratio of the layers changed in proportion to the mixing ratio of each spheres. In a glass dish, wave-like macroscopic drying patterns were observed in the intermediate areas between the outside edges of the broad ring and the inner wall of the cell. On a cover glass, the sphere mixing ratios were analyzed from the widths of the drying broad rings of the small spheres at the outside edge. High and distinct broad rings of small spheres and the low and vague broad one formed at the outer edges and in the inner area, respectively. Drying dissipative pattern was clarified to be one of the novel analysis techniques of colloidal size in binary colloidal mixtures.

Keywords Dissipative structure · Sedimentation pattern · Drying pattern · Binary suspension · Colloidal silica spheres · Colloidal size characterization · Broad ring pattern

T. Okubo (✉)
Institute for Colloidal Organization,
Hatoyama 3-1-112,
Uji 611-0012, Japan
e-mail: okubotsu@ybb.ne.jp

T. Okubo
Cooperative Research Center, Yamagata University,
Johnan 4-3-16,
Yonezawa 992-8510, Japan

J. Okamoto · A. Tsuchida
Department of Applied Chemistry, Gifu University,
Gifu 501-1193, Japan

Introduction

Most structural patterns in nature are formed via self-organization accompanied with the dissipation of free energy and in the non-equilibrium state. Among several factors in the free energy dissipation of aqueous colloidal suspensions, evaporation of solvent molecules at the air–solvent interface, and gravitational convection are very important. To understand the mechanisms of the dissipative self-organization of the simple model systems, instead of the much complex nature itself, the authors have studied the convectional, sedimentation, and drying dissipative patterns of suspensions and solutions.

Several papers on the drying pattern formation of the colloidal suspensions were reported so far [1–20]. Electrostatic interparticle interactions have been pointed out as one of the important factors for the dissipative structures. Hydrophobic and hydrophilic interactions between spheres were also demonstrated to be important in the drying processes [13–16]. Gelbart et al. [5, 7] examined the mechanism of solvent evaporation in the broad ring formation. Haw [17], Narita et al. [18], and Russel et al. [19] have studied the dynamic and phase transitional processes in dryness. Shimomura et al. and other researchers have studied the dissipative patterns in drying polymer solutions [20].

Recently, drying, sedimentation, and convectional dissipative patterns have been reported by authors for many kinds of suspensions and solutions, i.e., colloidal silica spheres, polystyrene spheres, plate-like fractionated bentonite particles, green tea, Chinese black ink, simple electrolytes, linear-type synthetic polyelectrolytes, water-soluble nonionic polymers, biopolymers, thermosensitive gels, detergents, and dyes for example [21–42]. The macroscopic broad ring patterns of the hill accumulated with solutes in the outside edges were always formed. For the nonspherical particles, the round hill was formed in the central area in addition to the broad ring. Macroscopic spoke-like cracks or lines were also observed for many solutes. The convectional flow of water and the solute molecules under gravity and the translational and rotational Brownian movement of the latter were important for the macroscopic pattern formation. Furthermore, so many types of beautiful microscopic fractal patterns such as branch-like, arc-like, block-like, star-like, cross-like, and string-like ones were observed on the microscopic scale. These microscopic drying patterns were reflected from the shape, size, and flexibility of the solute molecules themselves. Microscopic patterns also supported the importance of the electrostatic and the hydrophobic interactions between solutes and/or between the solutes and substrate during the course of solidification. One of the important findings in our experiments was that the primitive vague patterns formed already in the suspension state by convection before dryness, and they grew toward fine structures in the course of solidification.

The broad ring-like sedimentation patterns were formed so often in suspension state at room temperature by the convectional flow of water and the colloidal particles. The important finding in this study was that the sedimentary particles were suspended above the substrate and always moved in balancing the convectional flow with the sedimentation of the particles under the gravity.

Existence of the small circle-like cell convections ("*Saibo-uzu*" in Japanese), was proposed by Terada et al. for the first time [43–45]. Cell convections were observed by the authors for the suspensions of Chinese black ink on a cover glass. The spoke-like convectional patterns were observed for Chinese black ink on a water surface [43–45], Chinese black ink [25], and poly (methyl methacrylate) spheres (Okubo T, publication in preparation) on a cover glass. The convectional patterns of colloidal silica spheres in 100% ethyl alcohol changed dynamically with time [33]. Hexagonal circulating cells ("Bernard" cell) are also well known as one of the macroscopic convectional dissipative patterns [46].

It should be mentioned in this study that distinction of microstructures and macrostructures is arbitrary in our work hitherto because the dissipative patterns are stratified on microscales to macroscales. However, the authors often say that the patterns in the order larger than and smaller than 1 mm are macrostructures and microstructures, respectively.

In this work, sedimentation and drying dissipative patterns of the binary mixtures among the colloidal silica spheres, 183 nm, 305 nm, and 1.205 μm in diameter, have been studied on a watch glass, a glass dish, and a cover glass in the macroscopic and microscopic scales. One of the main purposes of this work is to develop a novel technique for size analysis of the colloidal mixtures from the dissipative structural patterns. It is highly plausible that the dissipative pattern method is developed as a unique and convenient technique of colloidal characterization in the near future.

Experimental

Materials

CS161, CS300, and CS1000A silica spheres were kindly donated from Catalysts and Chemicals (Tokyo). Diameters, SDs from the mean diameter, and polydispersity indices of the spheres were 183±18.6 nm and 0.10, 305±9.1 nm and 0.030, and 1.205 μm±14 nm and 0.012, respectively. These size parameters were determined from an electron microscope (Hitachi, H8100) in Gifu University. The CS300 and CS1000A spheres were carefully purified by repeated decantation more than 30 times. Then the samples including CS161 were treated on a mixed bed of cation-exchange and anion-exchange resins [BioRad, AG501-X8 (D), 20–50 mesh] more than 6 years before use because newly produced silica spheres always released a considerable amount of alkali ions from the porous sphere surfaces for a long time. Water used for the sample preparation was purified by a Milli-Q reagent grade system (Milli-RO5 plus and Milli-Q plus, Millipore, Bedford, MA, USA).

Observation of the dissipative structures

Of the aqueous suspensions of the silica samples, 4, 5, or 0.1 ml were put carefully and gently into a medium size watch glass (70 mm in diameter; TOP, Tokyo), a glass dish (42 mm in inner diameter and 15 mm in height, code 305-02; TOP, Tokyo), or a cover glass (30×30 mm, thickness no. 1, 0.12 to 0.17 mm; Matsunami Glass, Kishiwada, Osaka) set in a glass dish (60 mm in diameter and 15 mm in depth; Petri, Tokyo), respectively. The sedimentation and drying patterns were observed for the suspensions on a desk covered with a black plastic sheet until dried up completely in a room air-conditioned at 24±1 °C. The humidity of the room air was between 45% and 60%, which was not regulated. Total concentrations of the mixtures were kept to

be 0.01374 in volume fraction. The mixing ratios (x) of the two sphere components were 0, 0.2, 0.35, 0.5, 0.65, 0.8, and 1 for each combination.

Macroscopic dissipative structures were observed on a Canon EOS 10D digital camera (Canon, Tokyo) with a lens (EF 28–200 mm, f=3.5–5.6 USM, Canon). Microscopic structures were observed with a metallurgical microscope (PME-3, Olympus, Tokyo). Thickness profiles of the dried films were measured on a laser 3-D profile microscope (type VK-8500, Keyence, Osaka). Reflection spectra of the dried film were recorded on a High-sensitivity Spectrum Multi-channel Photo-detector (MCPD-7000 G3, Otsuka Electronics, Osaka) with a Y-type optical fiber. AFM (Atomic Force Microscopy) measurements were made on a Nano-scale Hybrid Microscope (type VN-8000, Keyence).

Results and discussion

Macroscopic sedimentation patterns of binary sphere mixtures

Figure 1 shows the sedimentation patterns of the mixtures of CS1000A and CS161 in a watch glass (a–e), a glass dish (f–j), and a cover glass (k–o). In a watch glass, the sedimentation areas of large spheres were small compared with those of small spheres in the suspension state 10 h or more after setting the suspensions. The gravitational sedimentation of the large spheres should be faster than that of small spheres. Furthermore, the convectional flow of the small spheres from center to the outside edges in the lower layers of the liquid should be fast compared with that of large spheres. Thus, the size segregation of the large and small spheres into the inner and outer regions is quite understandable. In a watch glass, the clear-cut broad ring-like sedimentation patterns were not observed with the naked eyes. However, the broad ring accumulation of the spheres in the suspension state is highly plausible from the broad ring formation in the drying patterns as described below and also from the broad rings observed in the sedimentation state for the single component sphere suspensions [32, 39, 40]. The broad ring-like sedimentation patterns were formed clearly in a glass dish (Fig. 1f–j). However, segregation of the small and large spheres cannot be observed with the naked eyes in the sedimentation state. On a cover glass, the broad ring-like sedimentation patterns where color changes from pinkish white to blue as the mixing ratio of the small spheres increased were observed clearly with the naked eyes (see Fig. 1k–o). Sedimentation patterns of binary mixtures of CS1000A+CS300 and CS300+CS161 were also observed and similar results to those of CS1000A+CS160 described above were obtained on a watch glass, a glass dish, and a cover glass. The pictures showing these were, however, omitted in this paper.

A main cause for the broad ring formation is due to the convectional flow of water and colloidal spheres in the different rates where motion of colloidal spheres are slower than water molecules under gravity. Furthermore, the convectional flow is clearly faster for smaller spheres. Especially, flow of the spheres from the center area toward

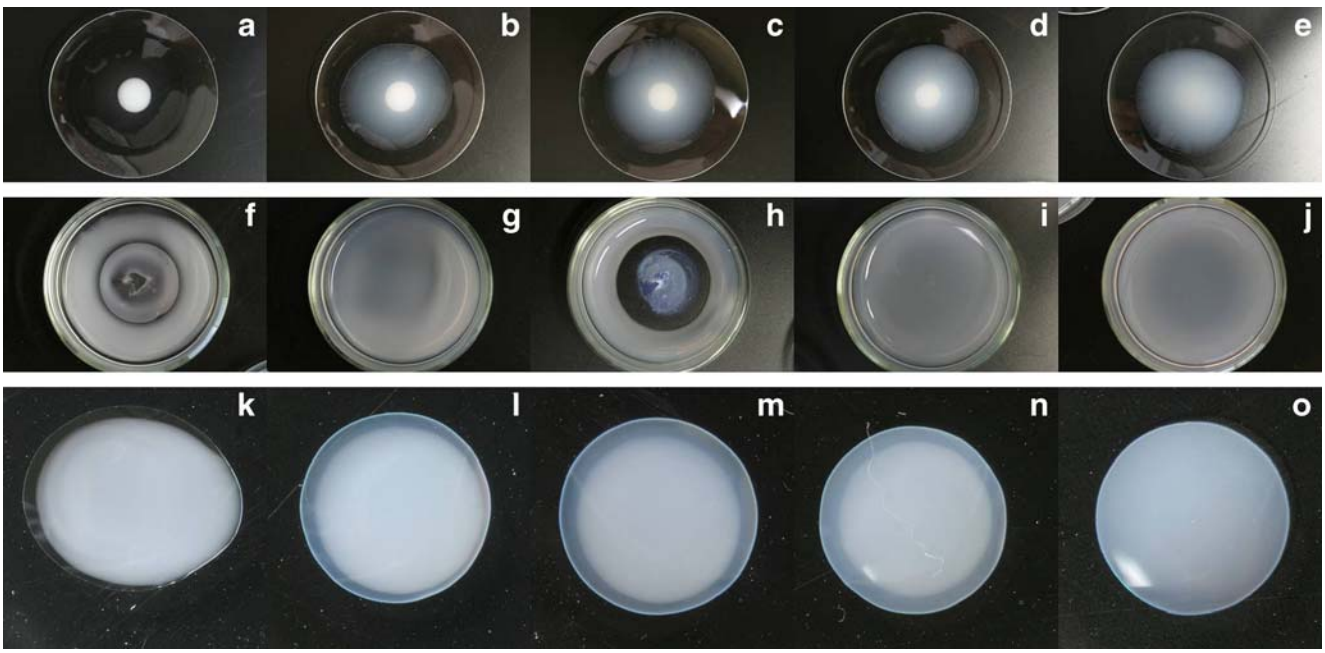

Fig. 1 Sedimentation patterns of mixed spheres CS1000A (component 1) + CS161 (3) in a watch glass (**a** to **e**, after 10 h and 30 m), a glass dish (**f** to **j**, after 44 h) and a cover glass (**k** to **o**, after 3 h) at 24 °C. **a**, **f**, **k** ϕ_1=0.0137, ϕ_3=0; **b**, **g**, **l** ϕ_1=0.0089, ϕ_3=0.0048; **c**, **h**, **m** ϕ_1=0.0069, ϕ_3=0.0069; **d**, **i**, **n** ϕ_1=0.0048, ϕ_3=0.0089; **e**, **j**, **o** ϕ_1=0, ϕ_3=0.0137

the outside edges in the lower layer of the liquid, which was observed for suspensions of Chinese black ink [25] in a glass dish and poly (methyl methacrylate) (Okubo T, publication in preparation) on a cover glass, is important. The convectional flow in a watch glass, for example, is enhanced by the evaporation of water at the liquid surface, resulting in the lowering of the suspension temperature in the upper region of the suspension. When the colloidal spheres reach the outside edges of the liquids, a part of the spheres will turn upward and go back to the center region. However, most of spheres will be accumulated at the outside edges by the downward flow of the spheres caused by gravitational sedimentation. Thus, the broad rings are formed at the outside edges.

It should be noted that the broad ring-like sedimentation patterns in the glass dish reported in this study were observed, for the first time, in a previous paper from the author's laboratory [32] as the authors know. However, the broad ring formation in the dried patterns has been so often observed for most of the suspensions and solutions examined so far by our group [21–42] and other researchers [1–20], irrespective of the cells used. It should be mentioned that the microgravity experiments were made for the observation of the drying dissipative patterns of deionized suspension of colloidal silica spheres [47]. It is surprising to note that the broad ring patterns still appeared even in microgravity. This supports strongly that both the gravitational and the Marangoni convections contribute to the broad ring formation on earth, and the latter is still important in microgravity.

We should note that the broad ring patterns are formed already in the process of convectional flow of water and solutes in suspension state. The broad ring-like sedimentation patterns have been observed in a polystyrene dish [31], in a watch glass [31], and even in a deep bowl [34]. It should be further noted that the sedimentary spheres, especially in a deionized suspension, are surrounded with the extended electrical double layers and move keeping apart from the cell wall, which is also surrounded by the electrical double layers.

Macroscopic drying patterns of binary sphere mixtures

Figures 2, 3, and 4 show the drying patterns of the binary mixtures of CS1000A+CS161, CS1000A+CS300 and CS300+CS161, respectively, in a watch glass (a to e), a glass dish (f to j), and a cover glass (k to o). In Fig. 2a–e, the main dried areas of large (CS1000A) and small spheres (CS161) were white and small and blue and large, respectively, in a watch glass. The dried patterns of the binary mixtures were composed of the outer broad layer of small spheres and the inner layer of large spheres. It is interesting to note that the width ratio (r) of each layers changed roughly in proportion to the mixing ratio (χ) of the small and large spheres as is shown in Fig. 5a. The r values increased in proportion to x for the three kinds of mixtures, though the experimental errors were rather large. Thus, analysis of the mixing ratio of each sphere is possible using a watch glass. The wave-like and slightly iridescent colored structures were formed in the intermediate areas between the outside edges of the broad

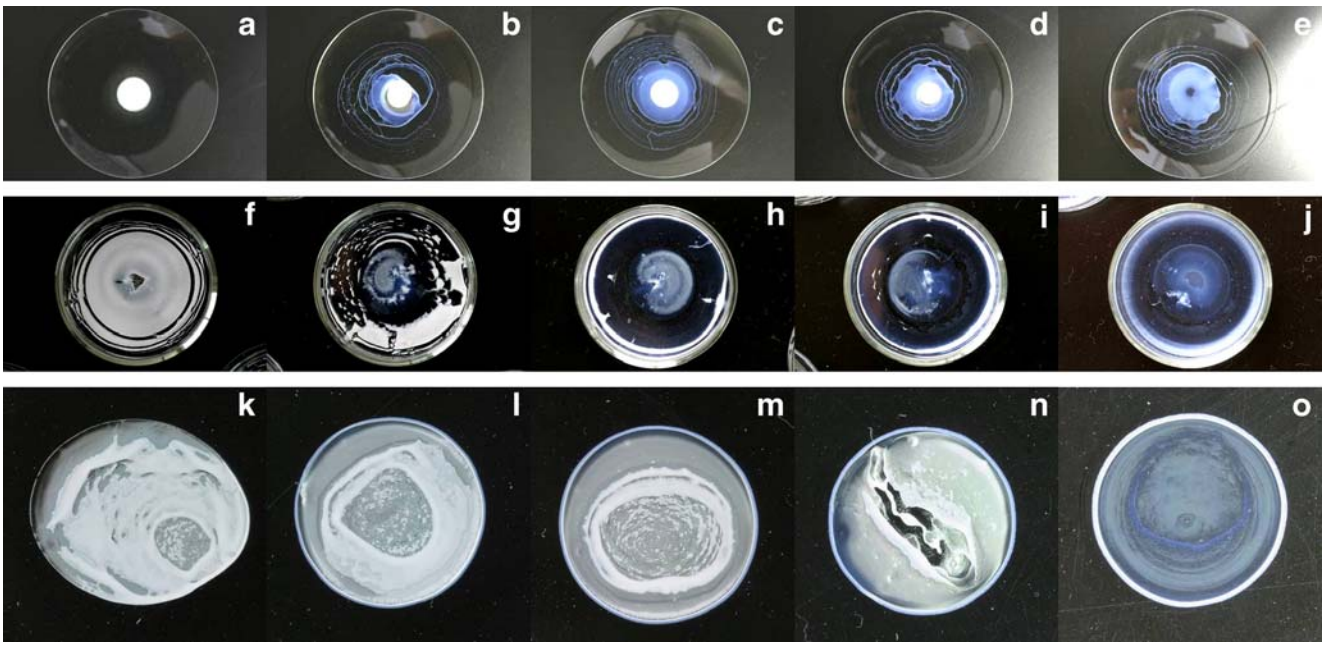

Fig. 2 Drying patterns of mixed spheres CS1000A (1)+CS161 (3) in a watch glass (**a** to **e**, after 33 h and 25 m), a glass dish (**f** to **j**, after 58 h and 40 m) and a cover glass (**k** to **o**, after 5 h) at 24 °C. **a**, **f**, **k** ϕ_1=0.0137, ϕ_3=0; **b**, **g**, **l** ϕ_1=0.0089, ϕ_3=0.0048; **c**, **h**, **m** ϕ_1=0.0069, ϕ_3=0.0069; **d**, **i**, **n** ϕ_1=0.0048, ϕ_3=0.0089; **e**, **j**, **o** ϕ_1=0, ϕ_3=0.0137

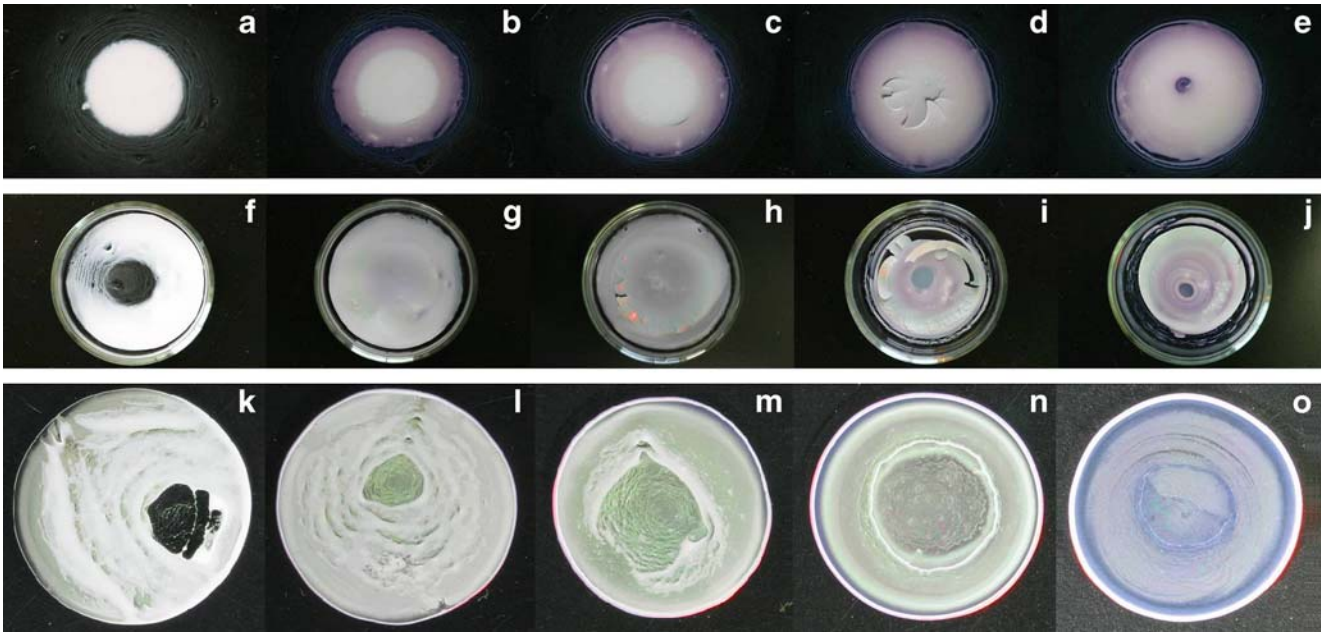

Fig. 3 Drying patterns of mixed spheres CS1000A (1)+CS300 (2) in a watch glass (**a** to **e**), a glass dish (**f** to **j**) and a cover glass (**k** to **o**) at 24 °C. **a**, **f**, **k** ϕ_1=0.0137, ϕ_2=0; **b**, **g**, **l** ϕ_1=0.0110, ϕ_2=0.00275; **c**, **h**, **m** ϕ_1=0.0069, ϕ_2=0.0069; **d**, **i**, **n** ϕ_1=0.00275, ϕ_2=0.0110; **e**, **j**, **o** ϕ_1=0, ϕ_2=0.0137

ring and the inner wall of a glass dish as is shown in Fig. 2g. The similar patterns were observed for the diluted suspensions of CS300 spheres for the first time [39]. The drying frontier started at the center of the glass dish and moved toward the outer cell wall with time. These wave-shaped patterns appeared only when the concentration of the spheres is not high enough to cover the spheres over the cell surfaces. On a cover glass, rather sharp broad rings were formed at the outside edges (see Fig. 2k–o). The broad rings at the outside edges in Fig. 2l–n are blue and their widths look to increase as the fraction of small spheres (χ) increases. Macroscopic observation of the dried film clarified that the

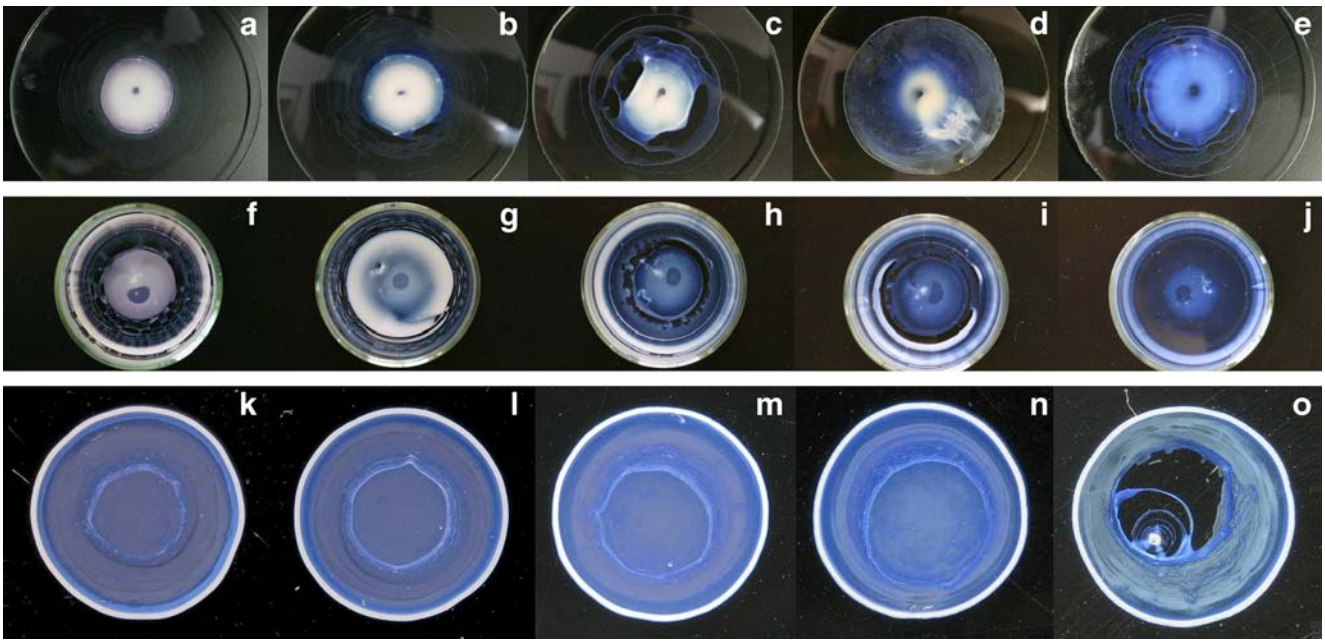

Fig. 4 Drying patterns of mixed spheres CS300 (2)+CS161 (3) in a watch glass (**a** to **e**, 4ml), a glass dish (**f** to **j**, 5 ml) and a cover glass (**k** to **o**, 0.1 ml) at 24 °C. **a**, **f**, **k** ϕ_2=0.0137, ϕ_3=0; **b**, **g**, **l** ϕ_2=0.0110, ϕ_3=0.00275; **c**, **h**, **m** ϕ_2=0.0069, ϕ_3=0.0069; **d**, **i**, **n** ϕ_2=0.00275, ϕ_3=0.0110; **e**, **j**, **o** ϕ_2=0, ϕ_3=0.0137

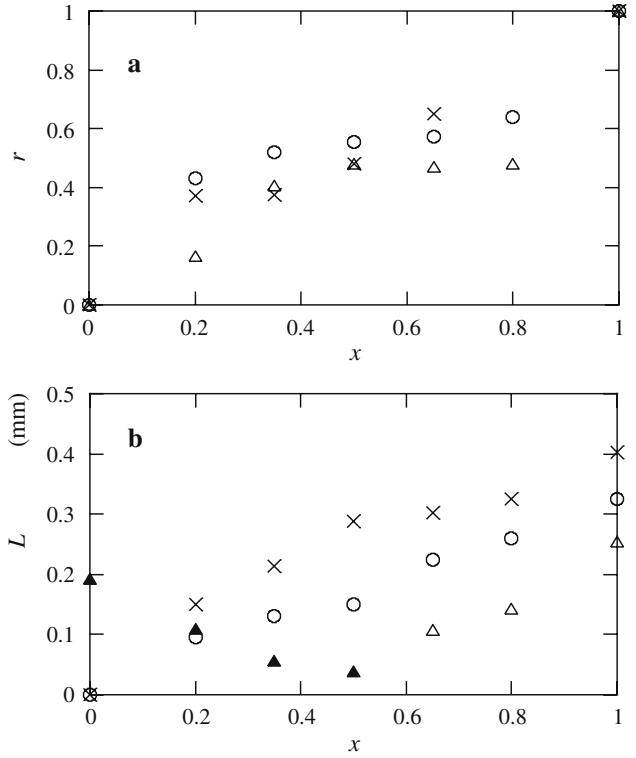

Fig. 5 **a** Width ratio (r) of the drying segregated areas in a watch glass as a function of the mixing ratio (x) in the binary mixtures. ◯ CS1000A (1)+CS161 (3), *X* CS1000A (1)+CS300 (2), *open triangles* CS300 (2)+CS161 (3). **b** Width of the broad rings (L) on a watch glass as a function of the mixing ratio (x) in the binary mixtures. ◯ CS161 (3) in CS1000A (1)+CS161 (3), *X* CS300 (2) in CS1000A (1)+CS300 (2), *open triangles* CS161 (3) in CS300 (2)+CS161 (3), *filled triangles* CS300 (2) in CS300 (2)+CS161 (3)

width of the broad ring increases in proportion to the x values, which will be discussed later in detail using Figs. 9 and 10 for microscopic observation. Furthermore, in Fig. 2m, a very wide and white broad ring was observed in the inner area of the dried film besides the sharp and blue broad ring at the outside edges.

Drying patterns of the binary mixtures of CS1000A+ CS300 spheres in a watch glass are shown in Fig. 3a–e. The main dried areas of CS1000A and CS300 were white and small and pink and large at the inner and outer layers, respectively. The width ratios again changed in proportion to the mixing ratios (see Fig. 5). In a glass dish, the broad rings were formed at the inner areas apart from the inner cell wall irrespective of the mixing ratio of CS1000 and CS300. On a cover glass, the rather sharp broad rings were observed irrespective of the mixing ratio. Again, sharp pink and very wide white broad rings were formed at the outside edge and inside area of the dried film in Fig. 3m. Coexistence of two broad rings was again supported by the width profile of the dried film, though the graph showing this was omitted here to save space.

Figure 4 shows the drying patterns on a watch glass, a glass dish, and a cover glass, respectively, as a function of the mixing ratio between CS300 and CS161. Size segregation on a watch glass is again clear, i.e., blue and pink (or whitey pink) layers were separated at the outside and inside, respectively. The reflection spectra of the dried films of CS300 and CS161 were taken on a watch glass as is shown in Fig. 6. Though the graphs showing the profiles are omitted in this paper, the peak wavelengths at the outer layer of the film of the mixtures of CS300+CS161 (code 371 corresponding to Fig. 4e, $\phi_2=0$, $\phi_3=0.0137$ where ϕ denotes the sphere concentration in volume fraction), at the outer layer of CS300+CS161 (code 373, $\phi_2=0.0048$, $\phi_3=0.0089$), at the inner layer of code 373, at the inside region of the inner layer of code 377 (corresponding to Fig. 4a, $\phi_2=0.0137$, $\phi_3=0$), and at the outside region of the inner layer of code 377 were 415, 560, 665, 665, and 665 nm, respectively. The nearest-neighbored intersphere distance (D) is estimated from the peak wavelengths (λ_p) using Eq. 1 [48]:

$$D = 0.6124\,(\lambda p/n) \tag{1}$$

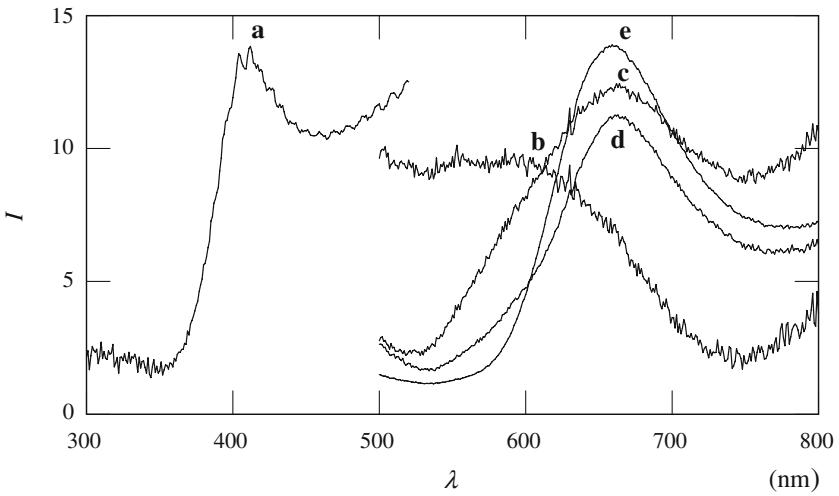

Fig. 6 Reflection spectra of the dried films of CS161 (1) (**a**), CS161 (1)+CS300 (2) (**b**, **c**) and CS300 (2) (**d**, **e**) in a watch glass at 25 °C. **a** Outside region, code 371, $\phi_1=0.0138$, $\phi_2=0$; **b** outer layer, code 373, $\phi_1=0.0089$, $\phi_2=0.0048$; **c** center region, code 373; **d** center region, code 377, $\phi_1=0$, $\phi_2=0.0138$; **e** outside region, code 377

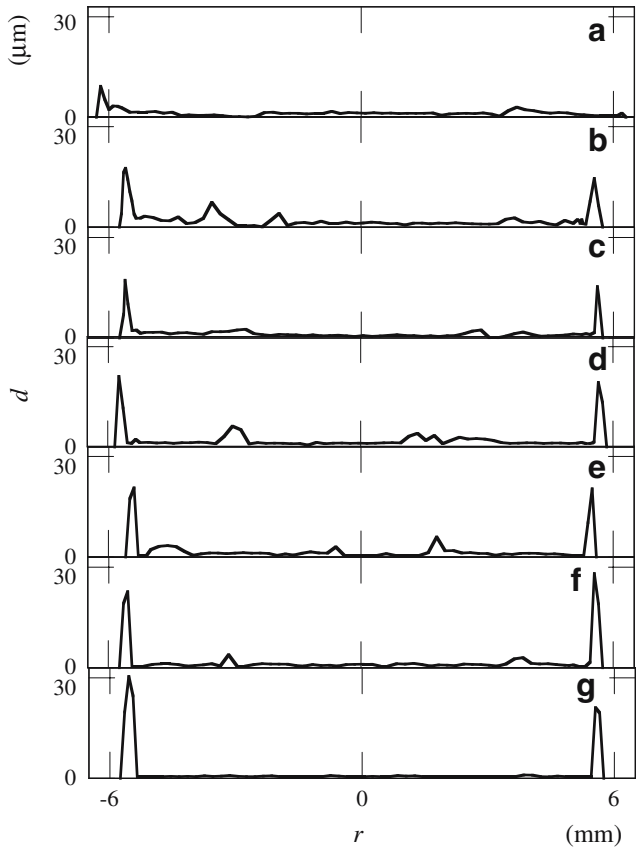

Fig. 7 Thickness profiles of the dried films of mixed spheres CS1000A (1)+CS161 (3) on a cover glass at 24 °C. **a** ϕ_1=0.0137, ϕ_3=0; **b** ϕ_1=0.0110, ϕ_3=0.0027; **c** ϕ_1=0.0089, ϕ_3=0.0048; **d** ϕ_1=0.0069, ϕ_3=0.0069; **e** ϕ_1=0.0048, ϕ_3=0.0089; **f** ϕ_1=0.0027, ϕ_3=0.0110; **g** ϕ_1=0, ϕ_3=0.0137

Here, the refractive index of dried film (n) is given by Eq. 2.

$$n = 0.74 \times [\text{refractive index of silica}] + 0.26 \times [\text{refractive index of air}] \quad (2)$$

Refractive indices of silica and air were assumed to be 1.5 and 1.00, respectively. Furthermore, the spheres in the dried film are assumed to be attached to each other and distribute in the closed-packed colloidal crystal structure. The D values of the dried film evaluated to be 180 and 288 nm using Eq. 1 from the values of λ_p, 415 and 665 nm, respectively. These D values agreed excellently with the diameters of CS161 and CS300 spheres, 183 and 305 nm, respectively. This agreement supports that the neighbored spheres are almost in contact to each other, keeping a crystal structure. Thus, the peak wavelengths of 415 and 665 nm are attributed to the colloidal crystal films of CS161 and CS300 spheres, respectively. Furthermore, the inner layer of the mixture (code 373) is occupied mostly with CS300 spheres, but also with CS161 in part. However, the outside layer is occupied with CS161 exclusively.

On a cover glass, two broad rings were also observed for the mixtures of CS300 and CS161 as is shown in Fig. 4m. The sharp and white broad ring at the outside edge and the wide and pinky white broad ring at the inner area are assigned to the accumulation of CS161 and CS300 spheres, respectively, again with help of the thickness profile of the dried film. However, peak wavelengths in the reflection

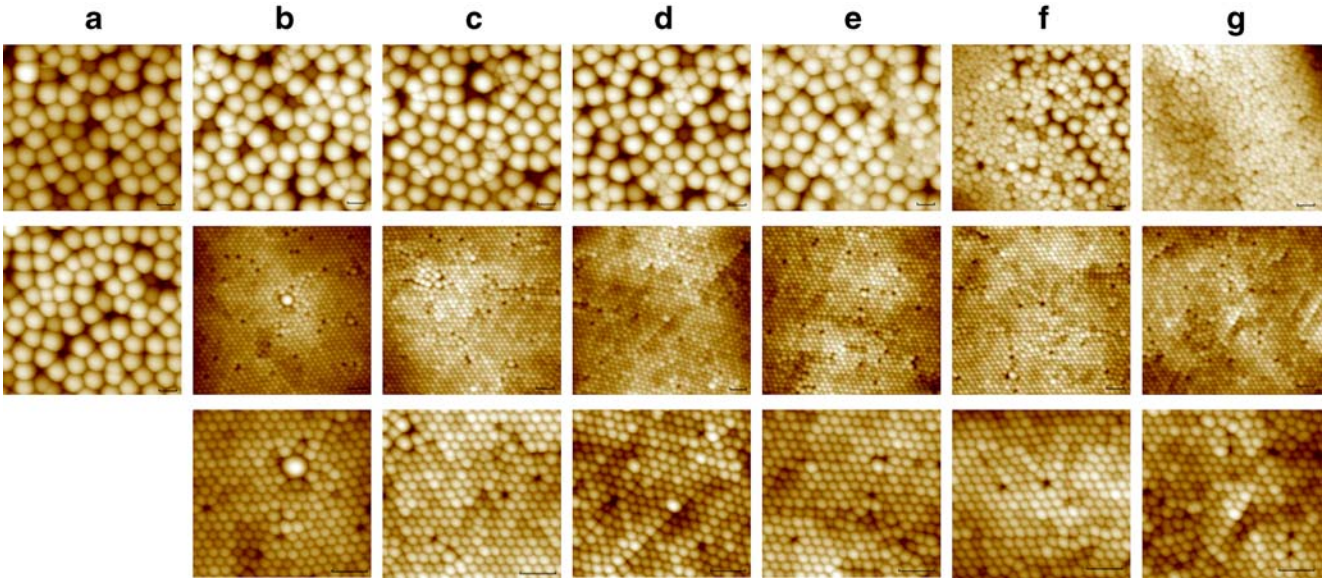

Fig. 8 AFM observation of the dried films of mixed spheres CS1000A (1)+CS300 (2) on a cover glass at 24 °C. **a** ϕ_1=0.0137, ϕ_2=0; **b** ϕ_1=0.0110, ϕ_2=0.00275; **c** ϕ_1=0.0089, ϕ_2=0.00480; **d** ϕ_1=0.0069, ϕ_2=0.0069; **e** ϕ_1=0.00482, ϕ_2=0.0089; **f** ϕ_1=0.00275, ϕ_2=0.0110; **g** ϕ_1=0, ϕ_2=0.0137. *Top frames* air–film interface area of the inner broad ring, scan area=10×10 μm; *middle frames* outer edge broad ring, scan area=10×10 μm; *bottom frames* outer edge broad ring, scan area=5×5 μm

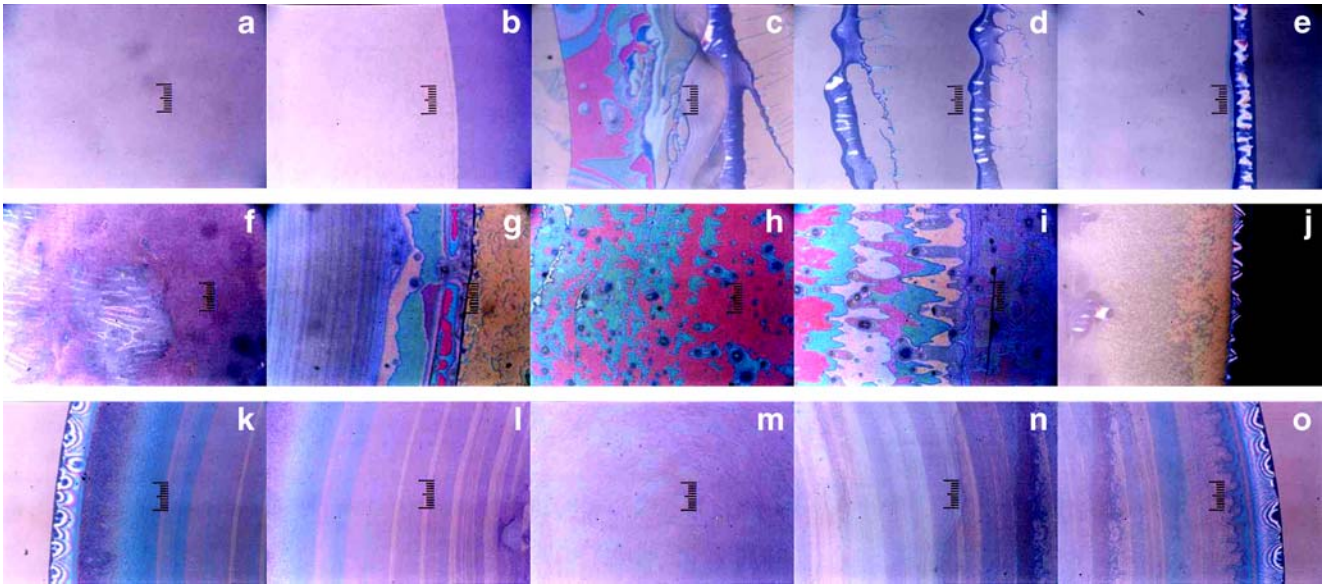

Fig. 9 Microscopic drying patterns of mixed spheres CS1000A (1)+ CS161 (3) in a watch glass (**a** to **e**, after 33 h and 25 min, 4 ml), a glass dish (**f** to **j**, after 58 h and 40 min, 5 ml) and a cover glass (**k** to **o**, after 6 h and 10 min, 0.1 ml) at 24 °C. $\phi_1 = \phi 3 = 0.0069$, from the center (**a**, **f**) to the right edge (**e**, **j**), from the left edge (**k**) to the right edge (**o**), full scale is 0.2 mm

spectroscopy supported existence of the dried crystals of CS161 spheres only, though the peak profiles showing this are omitted in this report. This will be partly due to the fact that the colloidal crystals of CS161 coexist even in the area of the wide broad ring of CS300 spheres.

Thickness profiles of the dried film for CS1000A and CS161 mixtures on a cover glass are shown in Fig. 7. The sharp broad ring of small CS161 spheres, approximately 30 μm in height (see Fig. 7g) appeared at the outside edges. On the other hand, the height of the broad ring of large CS1000A spheres was low, approximately 10 μm or lower, and the large spheres distributed almost everywhere besides the broad ring area (see Fig. 7a). For the mixtures, coexistence of the rather sharp principal broad rings and low and wide ones is clear at the outside edges and the inner area, respectively. It is interesting to note that the

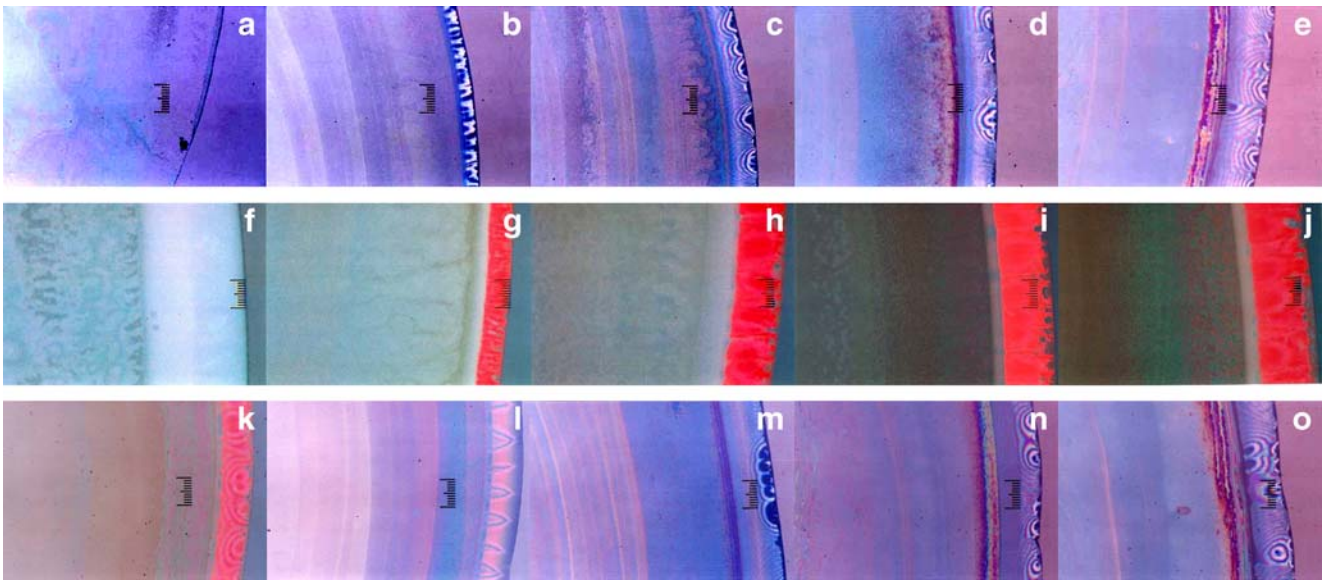

Fig. 10 Microscopic drying patterns of mixed spheres CS1000A (1)+ CS161 (3) (**a** to **e**), CS1000A (1)+CS300 (2) (**f** to **j**) and CS300 (2)+ CS161 (3) (**k** to **o**) on a cover glass at 24 °C. 0.1 ml, **a** $\phi_1 = 0.0137$, $\phi_3 = 0$; **b** $\phi_1 = 0.0110$, $\phi_3 = 0.00275$; **c** $\phi_1 = 0.0069$, $\phi_3 = 0.0069$; **d** $\phi_1 = 0.00275$, $\phi_3 = 0.0110$; **e** $\phi_1 = 0$, $\phi_3 = 0.0137$; **f** $\phi_1 = 0.0137$, $\phi_2 = 0$; **g** $\phi_1 = 0.0110$, $\phi_2 = 0.00275$; **h** $\phi_1 = 0.0069$, $\phi_2 = 0.0069$; **i** $\phi_1 = 0.00275$, $\phi_2 = 0.0110$; **j** $\phi_1 = 0$, $\phi_2 = 0.0137$; **k** $\phi_2 = 0.0137$, $\phi_3 = 0$; **l** $\phi_2 = 0.0110$, $\phi_3 = 0.00275$; **m** $\phi_2 = 0.0069$, $\phi_3 = 0.0069$; **n** $\phi_2 = 0.00275$, $\phi_3 = 0.0110$; **o** $\phi_2 = 0$, $\phi_3 = 0.0137$, after 6 h and 10 min, dry, at the right edge, full scale is 0.2 mm

latter looks to locate closer to the center of the film when the mixing ratio is closer to 0.5. Thus, the broad rings are composed of the sharp and broad ones corresponding to the small and large spheres at the outermost edge and the inner side, respectively, which is further supported from the macroscopic observation shown in Fig. 2m described above and further from the microscopic observation of the dried films as described below. Thickness profiles of the dried films of CS1000A+CS300 and CS300+CS161 mixtures were also measured. Coexistence of the sharp and wide, and low broad rings was again observed at the outside edges and the inner area, and they are assigned to the accumulations of small and large spheres, respectively.

Figure 8 shows the AFM observation of the air–film interface of the dried films of the sphere mixtures CS1000A and CS300 on a cover glass. The segregation of the large and small spheres toward the inner and the outside broad rings is very clear as the authors expected before the observation. The significant segregation among the two different sizes of spheres was also supported from the AFM observations of CS1000A+CS160 and CS300+CS160 mixtures, though the segregation for the latter system was not so perfect compared with those for CS1000A+CS160 and CS1000A+CS300 mixtures. Showing of the AFM pictures of the mixtures CS1000+CS160 and CS300+CS160 were omitted in this article to save space.

Microscopic drying patterns of binary sphere mixtures

Figure 9 shows the microscopic observation of the CS1000A+CS161 mixtures on a watch glass (from center to right edge), a glass dish (from center to right edge), and a cover glass (from left to right edges). On a watch glass, clear-cut border between CS1000A at central (pink region in Fig. 9b) and CS161 (blue region also in Fig. 9b) at outside regions is observed. Microstructures of fine multiple rings are shown in Fig. 9c–e. In a glass dish, very fine layered and array of islands-like patterns were observed. On a cover glass, fine layered structure was formed at the outside regions. However, assignment of each layers to the small or large spheres is impossible except the blue broad rings at the outside edges, which are assigned to the small CS161 spheres. The microscopic patterns of other mixtures, CS1000A+CS300, and CS300+CS161 were also very similar to the patterns of CS1000A+CS161, and the graphs showing these are omitted in this paper.

Figure 10 shows the typical examples of the microscopic pictures on a cover glass for CS1000A+CS161 (a–e), CS1000A+CS300 (f–j) and CS300+CS161 (k–o) mixtures at the outside areas of the dried films including the broad rings. It is surprising to note that the broad rings at the outermost edges are colored corresponding to the smaller spheres of the mixtures, i.e., blue (CS161) or red (CS300). Furthermore, the width of the broad rings (L) increased in proportion to the mixing ratio of the smaller spheres increased. Especially for mixtures of CS1000A and CS300, the width of the white broad rings corresponding to the larger sphere CS1000A also decreased as the mixing ratio of CS1000A decreased (see Fig. 10f–j). Figure 5b shows the plots of the L values estimated from the microscopic pictures against χ. The proportionality between L and χ is excellent. Thus, it is clear that the mixing ratio is also analyzed from the width of the outermost broad rings, when the binary mixtures are dried on a cover glass.

Summarizing the results, analysis of the mixing ratio is possible from (a) the width ratio of the colored layers of the dried films in a watch glass and (b) the width of the outermost broad rings corresponding to the smaller spheres on a cover glass. The coexistence of the sharp broad ring at the outside edges and wide hill-like one in the inner area will be also interesting in relation to the mixing ratio analysis. Careful observation of the dried patterns should afford further information, which is effective for analyses of mixing ratio and colloidal size.

Acknowledgments Financial supports from the Ministry of Education, Culture, Sports, Science and Technology, Japan and the Japan Society for the Promotion of Science are greatly acknowledged for the grants-in-aid for exploratory research (17655046) and scientific research (B) (18350057 and 19350110-0001), respectively. Catalysts and Chemicals is thanked deeply for providing the colloidal silica sphere samples.

References

1. Vanderhoff JW, Bladford EB, Carrington WK (1973) J Polym Sci Polym Symp 41:155
2. Nicolis G, Prigogine I (1977) Self-organization in non-equilibrium systems. Wiley, New York
3. Cross MC, Hohenberg PC (1993) Rev Mod Phys 65:851
4. Adachi E, Dimitrov AS, Nagayama K (1995) Langmuir 11:1057
5. Ohara PC, Heath JR, Gelbart WM (1998) Langmuir 14:3418
6. Uno K, Hayashi K, Hayashi T, Ito K, Kitano H (1998) Colloid Polym Sci 276:810
7. Gelbart WM, Sear RP, Heath JR, Chang S (1999) Faraday Discuss Chem Soc 112:299
8. van Duffel B, Schoonheydt RA, Grim CPM, De Schryver FC (1999) Langmuir 15:957
9. Maenosono S, Dushkin CD, Saita S, Yamaguchi Y (1999) Langmuir 15:957
10. Brock SL, Sanabria M, Suib SL, Urban V, Thiyagarajan P, Potter DI (1999) J Phys Chem 103:7416
11. Nikoobakht B, Wang ZL, El-Sayed MA (2000) J Phys Chem 104:8635
12. Ge G, Brus L (2000) J Phys Chem 104:9573
13. Chen KM, Jiang X, Kimerling LC, Hammond PT (2000) Langmuir 16:7825
14. Lin XM, Jaenger HM, Sorensen CM, Klabunde KJ (2001) J Phys Chem 105:3353
15. Kokkoli E, Zukoski CF (2001) Langmuir 17:369

16. Ung T, Liz-Marzan LM, Mulvaney P (2001) J Phys Chem 105:3441
17. Haw MD, Gilli M, Poon WCK (2002) Langmuir 18:1626
18. Narita T, Beauvais C, Hebrand P, Lequeux F (2004) Eur Phys J E 14:287
19. Tirumkudulu MS, Russel WB (2005) Langmuir 21:4938
20. Shimomura M, Sawadaishi T (2001) Curr Opin Colloid Interface Sci 6:11
21. Okubo T, Okuda S, Kimura H (2002) Colloid Polym Sci 280:454
22. Okubo T, Kimura K, Kimura H (2002) Colloid Polym Sci 280:1001
23. Okubo T, Kanayama S, Ogawa H, Hibino M, Kimura K (2004) Colloid Polym Sci 282:230
24. Okubo T, Kanayama S, Kimura K (2004) Colloid Polym Sci 282:486
25. Okubo T, Kimura H, Kimura T, Hayakawa F, Shibata T, Kimura K (2005) Colloid Polym Sci 283:1
26. Okubo T, Yamada T, Kimura K, Tsuchida A (2005) Colloid Polym Sci 283:1007
27. Yamaguchi T, Kimura K, Tsuchida A, Okubo T, Matsumoto M (2005) Colloid Polym Sci 283:1123
28. Kimura K, Kanayama S, Tsuchida A, Okubo T (2005) Colloid Polym Sci 283:898
29. Okubo T, Shinoda C, Kimura K, Tsuchida A (2005) Langmuir 21:9889
30. Okubo T, Yamada T, Kimura K, Tsuchida A (2006) Colloid Polym Sci 284:396
31. Okubo T (2006) Colloid Polym Sci 284:1395
32. Okubo T (2006) Colloid Polym Sci 284:1191
33. Okubo T (2006) Colloid Polym Sci 285:225
34. Okubo T (2006) Colloid Polym Sci 285:331
35. Okubo T, Itoh E, Tsuchida A, Kokufuta E (2006) Colloid Polym Sci 285:339
36. Okubo T, Nozawa M, Tsuchida A (2007) Colloid Polym Sci 285:827
37. Okubo T, Kimura K, Tsuchida A (2007) Colloids Surf 56:201
38. Okubo T, Onoshima D, Tsuchida A (2007) Colloid Polym Sci 285:999
39. Okubo T, Okamoto J, Tsuchida A (2007) Colloid Polym Sci 285:967
40. Okubo T (2007) Colloid Polym Sci 285:1495
41. Okubo T, Nakagawa N, Tsuchida A (2007) Colloid Polym Sci 285:1247
42. Okubo T, Yokota N, Tsuchida A (2007) Colloid Polym Sci 285:1257
43. Terada T, Yamamoto R, Watanabe T (1934) Proc Imp Acad Tokyo 10:10
44. Terada T, Yamamoto R, Watanabe T (1934) Sci Pap Inst Phys Chem Res 27:75
45. Terada T, Yamamoto R (1935) Proc Imp Acad Tokyo 11:214
46. Ball P (1999) The self-made tapestry formation in nature. Oxford University Press, Oxford
47. Tsuchida A, Okubo T (2003) Sen'i Gakkaishi 59:264
48. Okubo T (1986) J Chem Soc Faraday Trans 1(82):3175